Minerals Engineering 130 (2019) 36–47

Contents lists available at ScienceDirect

Minerals Engineering

journal homepage: www.elsevier.com/locate/mineng

Investigation on the flotation recovery of copper sulphosalts through an integrated mineralogical approach

Jonathan Rincon[a], Stoyan Gaydardzhiev[a,*], Lachezar Stamenov[b]

[a] University of Liege, GeMMe – Minerals Engineering and Recycling, Sart-Tilman Campus-B52, 4000 Liège, Belgium
[b] Dundee Precious Metals Chelopech, 2087 Village of Chelopech, Bulgaria

ARTICLE INFO

Keywords:
Geometallurgy
Copper sulphosalts
Flotation
Principal component analysis
Automated mineralogy

ABSTRACT

Investigation on the flotation behaviour of enargite (Cu_3AsS_4) and tennantite ($(Cu, Fe)_{12}As_4S_{13}$) during selective copper flotation was performed using an integrated mineralogical approach. To this end, samples taken from a production block at the Chelopech mine were subjected to a laboratory scale flotation and products characterized through multi-element chemical analyses and mineral mapping using a SEM-based automated mineralogy. Chemistry, modal mineralogy, copper-sulphosalts' liberation and associations were quantified. Principal component analysis (PCA) was employed to look for relationships between mineralogical features and flotation recovery. High variability in head copper grade was observed in the studied block, with deportment results attributing it to the varied content of enargite and tennantite. Chalcopyrite content was low in the majority of the samples. The close association and the frequently observed interlocking of pyrite and Cu-sulphosalt grains can explain pyrite (and gold) recovery during copper cleaner flotation. Linear equations based on PCA results allow the prediction of Cu-sulphosalts' recovery with a root mean square error of ± 1.32%.

1. Introduction

Geometallurgical modelling methodologies based on process mineralogy tools have been applied for flotation circuit optimization, problem solving and production forecasting through transforming traditional elemental grade control in block models to mineralogical oriented ones (Keeney and Walters, 2009; Lishchuk, 2016; Ntlhabane et al., 2018; Tungpalan et al., 2015a). Smith et al. (2013) and Dzvinamurungu et al. (2013), have assessed recovery and grade variations in PGM flotation in different Merensky Reef facies. Improved flotation recovery was facilitated by the higher degree of liberation of base metal sulphides (BMS), higher BMS content and lower orthopyroxene (Lotter et al., 2008) content, the latter being considered detrimental to PGM flotation. Wang and Fornasiero (2010), on the other hand, showed that increasing grain size of the target (floatable) mineral phase leads to decreased recoveries. Moreover, they found that particles with complex locking show higher flotation recoveries than particles with simple locking inside the same liberation and size class. This was especially observed in particles with lower liberation degrees and coarser grain sizes, being attributable to the higher probability of bubbles attaching to the hydrophobic patch in composite particles with complex locking rather than in those with simple locking (Farrokhpay and Fornasiero, 2017). The classification of mineral deposits following geometallurgical methodologies in which sampling, geological characterization and metallurgical test work are performed, offers a much clearer understanding of the processes needed for treating ore resources (Lotter, 2011; McKay et al., 2007; Whiteman et al., 2016). Lotter et al. (2011) described the important role of process mineralogy in the definition of six geometallurgical units at Glencore's Nickel Rim project, following textural and mineralogical characteristics, host rock relationships, mineral chemistry and PGM grades. Research results allowed the implementation of a flexible concentration flowsheet optimized to each unit without scarifying metallurgical performance. Whiteman et al. (2016), described the importance of using process mineralogy in the modelling and simulation of the flotation flowsheet of the Kamoa project, Democratic Republic of the Congo. The modelled flowsheet was confirmed through intensive experimental work that allowed the increase of Cu recovery and the decrease of SiO2 grade in the final concentrate, making it more suitable for conventional smelting techniques.

Flotation models based on mineralogical features have been developed by several authors, such as Tungpalan et al. (2015a, 2015b) who demonstrated that grain size distributions of copper sulphides can be used as a practical parameter to model flotation recovery. Ntlhabane et al. (2018) proposed a modelling framework which can be used as a decision making tool by companies. Their methodology included the

* Corresponding author.
E-mail address: S.Gaydardzhiev@ulg.ac.be (S. Gaydardzhiev).

https://doi.org/10.1016/j.mineng.2018.10.006
Received 7 June 2018; Received in revised form 25 August 2018; Accepted 8 October 2018

use of available process mineralogy tools such as SEM-based automated mineralogy to characterize feed and flotation products while assessing acid rock drainage (ARD) potential of flotation tailings. Furthermore, it was possible to demonstrate that such methodologies are a powerful tool for environmental impact and economic performance assessment. Zhang and Subasinghe (2016) created a predictive model for the recovery of sulphides (chalcopyrite, pyrite and sphalerite ± pyrrhotite) based on liberation, size and grade class' characteristics. The model provided high accuracy in calculating flotation recoveries within each size, grade and liberation class. Suazo et al. (2010) modelled flotation kinetics constants at the Collahuasi flotation circuit through varying particle size, gas flow rate and agitation. An intrinsic floatability parameter was proposed for each geometallurgical unit at the Rosario deposit (Chile). It was shown that information about the ore, such as lithology, alteration zones and mineralogy do influence flotation kinetics. Model results allowed forecasting copper recoveries at the concentrator with high accuracy.

During 2017 around 1.1 Mt ore were mined at the Chelopech mine, resulting in about 99,800 oz of gold and 7620 t of copper being concentrated through a flotation circuit comprising selective copper and pyrite cleaning stages, coupled to a SAG milling unit (Dundee Precious Metals Inc., 2017). Several geometallurgy–oriented studies aimed at improving metallurgical results and company revenues were recently initiated. Mena (2015) and Naumov (2016) reported results from series of flotation plant surveys and laboratory flotation tests at different operational regimes. SEM-based mineralogy was used to explain flotation behaviour and assess metallurgy. The findings have resulted in optimization of mineral concentration circuit with special attention to kaolinite group minerals and also suggestions on mixed collectors to improve selectivity at the bulk sulphide flotation phase.

The current work is a logical continuation in line with the above efforts and has an objective to link the mineralogical features of representative samples taken from a production block to the results achieved at laboratory scale flotation, with the final aim to predict the recovery of the main copper minerals via mathematical equations. The chosen methodology relies on implementation of the principal component analysis for linking flotation recovery to key mineralogical characteristics such as modal mineralogy, grain size and liberation degree.

2. Materials and methods

The research framework utilized in this study was adapted from existing geometallurgical modelling methodologies (Keeney and Walters, 2009; Keeney, 2010; Lopera Montoya, 2014; Tungpalan et al., 2015a). Fig. 1 illustrates the experimental pattern being followed, which consist of mineralogical characterization of selected samples from a production block at the Chelopech mine and their subsequent laboratory scale flotation. The obtained flotation products were further assayed for chemistry and submitted to automated mineralogy. Metallurgical performance and mineral characteristics were correlated using principal component analysis (PCA) to create linear models that were used to predict flotation performance. The methodology also included comminution testing procedures to characterize the samples in view resistance to impact breakage (drop weight tests) and grindability (batch grinding tests), however they are not reported here.

2.1. Geology and mineralogical characteristics of the Chelopech deposit

The Chelopech copper–gold deposit is located in the Panagyurishte metallogenic district, in the central part of the Srednogorie zone (Fig. 2). It was formed as a result of successive Late-Cretaceous accretion of volcanic island arcs (Stoykov et al., 2004). The Panagyurishte metallogenic district is composed by Precambrian basement of granitoids gneisses that were intruded by Paleozoic granitoids and overlain by upper – Cretaceous volcano-sedimentary sequences (Fig. 2). At the top of the sequence, Paleogene – Neogene foreland sediments overlay some parts of the Cretaceous formations (Chambefort and Moritz, 2014; Moritz et al., 2005).

Host of the mineralization is the 2000 m – thick Chelopech formation subdivided in lower and upper units. The lower unit hosts the mineralization with epithermal high sulfidation alteration zones (Georgieva and Hikov, 2016). It could be described as a central zone with high grade of copper and gold, surrounded by a silica halo of lower grade. The central zone possesses stockwork and massive sulphide mineralization, whereas the external halo is constituted by disseminated sulphides and silica overprinting (Georgieva et al., 2002; Moritz et al., 2005). These two zones present the boundaries for estimation of the Mineral Resources and are referred to as "Stockwork" and "Silica Envelopes". The mineralization is controlled by the argillic alteration halo which surrounds it. Alunite super group minerals as well as the kaolinite group minerals are considered important for exploration (Georgieva et al., 2002; Georgieva and Velinova, 2014). The ore body occurs in different morphologies encompassing lens-like, pipe-like and columnar, dipping steeply to the south - Fig. 2. The Chelopech deposit was classified as a volcanic – hosted massive sulphide deposit (VHMS), however latest findings suggest an epigenetic origin with replacement of volcanic rocks (Chambefort and Moritz, 2014; Stoykov et al., 2004).

It should be noted, that the copper sulphosalts constitute the major copper bearing minerals in the deposit followed by chalcopyrite ($CuFeS_2$). Therefore, the metallurgical behavior of the copper sulphosalts (throughout this article the term Cu-sulphosalts refers to enargite,

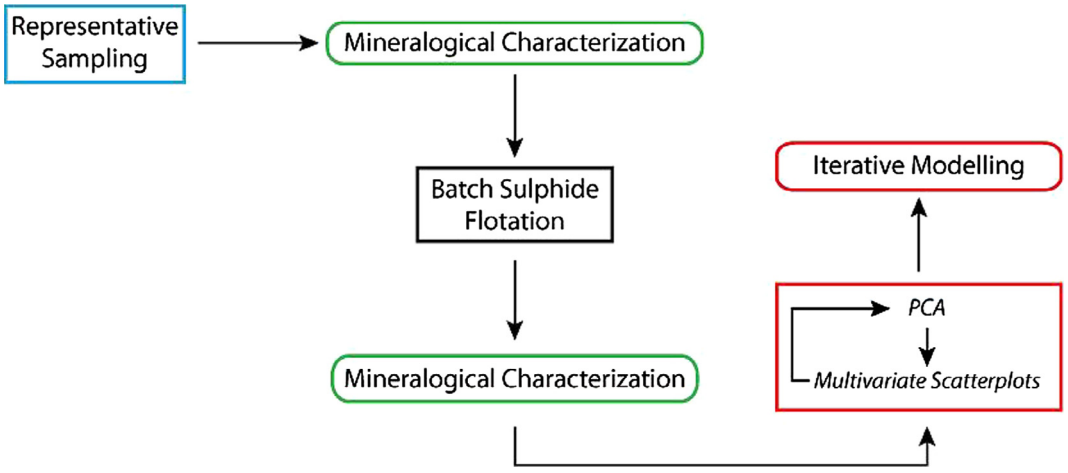

Fig. 1. Conceptual pattern of a geometallurgical characterization (adapted from Keeney (2010)).

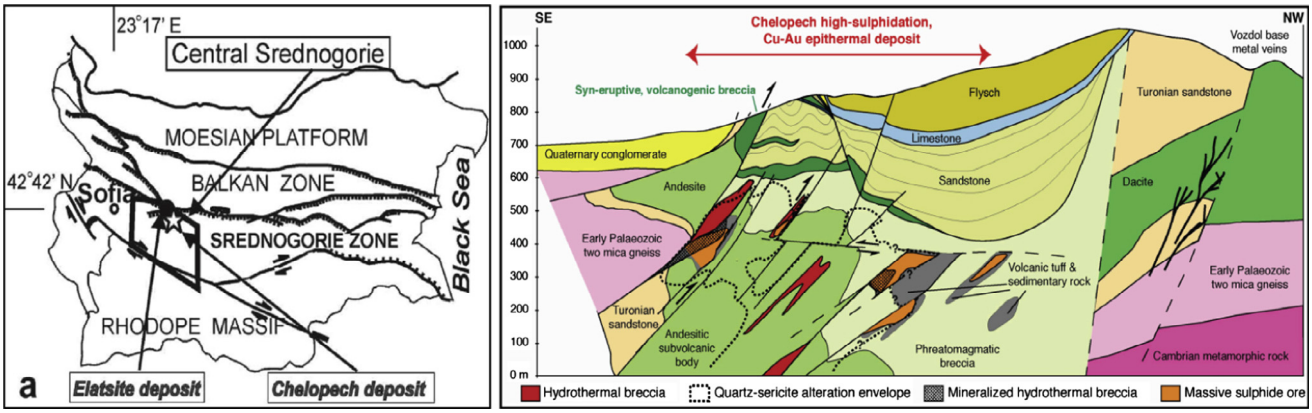

Fig. 2. Localization of the Chelopech project within the main Bulgarian geodynamic environments (left), and NW-SE profile with local geology and ore bodies (modified from Moritz et al., 2005; Stoykov et al., 2004).

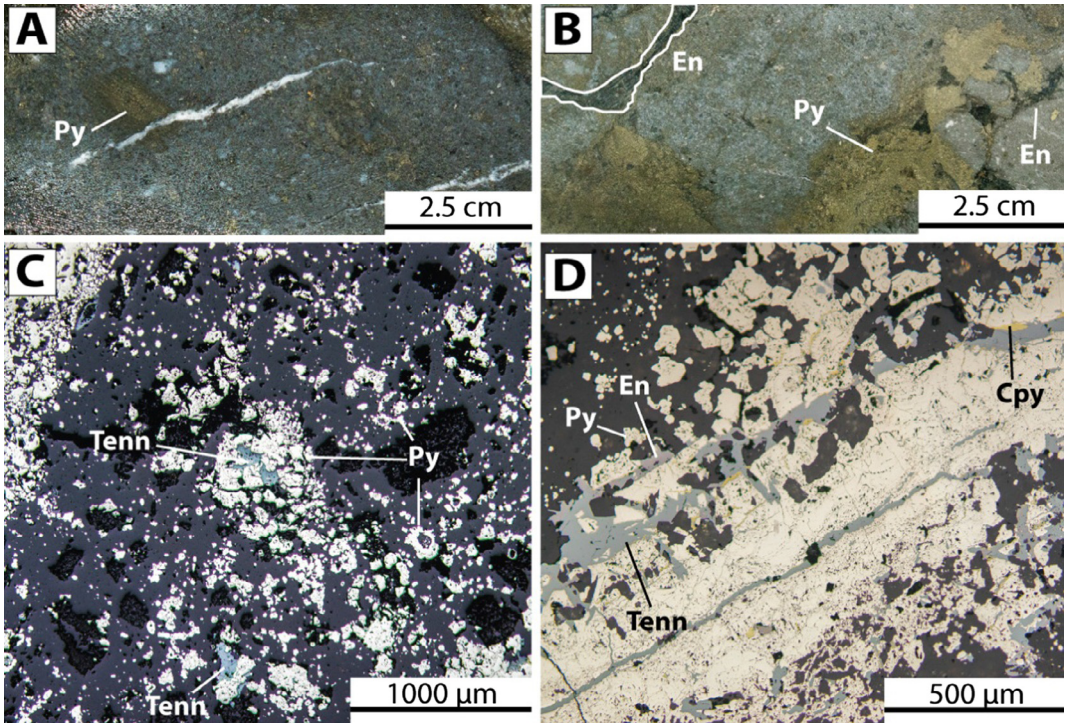

Fig. 3. A. Disseminated sulphide texture in volcanic tuff with quartz veins – image of Sample 6. B. stockwork texture in brecciated tuff in Sample 4. C. Microphotograph of disseminated sulphides texture in Sample 6 exhibiting pyrite-tennantite interlocking. D. Microphotograph of stockwork texture in Sample 4 showing tennantite, enargite and chalcopyrite in association with pyrite.

luzonite and tennantite), dictates the pay-metals for the mine. These are tennantite and enargite (including polymorph luzonite), which are complex minerals that combine a simple cation (typically $As^{3+,5+}$) and a metal cation (typically $Cu^{1+,2+}$ or Fe^{2+}) with a complex anion (typically S^{2-}) (Moëlo et al., 2008).

2.2. Block sampling and ore characteristics

The block under investigation was sampled at 10 different locations enabling to collect 6 drill core samples and 4 hand-picked samples at the tunnel development faces. For the latter, a sampling grid was implemented on the tunnels' advance front covering the targeted area. An average mass of 30 kg was gathered per sample, aiming to guarantee samples representativeness in terms of texture, mineralization style and lithology of each sampled region. Each sample was then crushed and homogenized and subsequently ground to 99% passing 6 mm and homogenized one more time. Finally, quartering was done to subsample 1.3 kg increments reserved for flotation tests. Each 1.3 kg sub-sample was evaluated following Gy's sampling theory (Gy, 1976), considering a sample lot of 30 kg and enargite and tennantite as target minerals. The variances were calculated following Eq. (1), using an established methodology (Gy, 1995, 1976)

$$\sigma^2(FSE) = \left(\frac{1}{Ms} - \frac{1}{Ml}\right) fg\beta cd^3 \quad (1)$$

where

f: shape factor,
g: particle size distribution factor,
β: liberation parameter,
d: size of the largest particle.

The variances obtained for all the samples were below 1.98×10^{-11} and the fundamental sampling error (FSE) was

8.89×10^{-6}.

The samples collected as flotation feeds were initially inspected using reflected light optical microscope. Pyrite was found as the most common opaque mineral within all the samples, commonly associated with enargite and/or tennantite presenting subhedral to euhedral crystals. Anhedral forms were observed as well. Locked crystals of pyrite were often associated with translucent gangue and other sulphides. Pyrite presented binary to more complex associations with all copper bearing minerals. Crystal sizes were about 40–60 μm in average. Enargite and tennantite are the second most common opaque minerals, usually found in binary associations between them and in ternary associations with pyrite and chalcopyrite, with sizes in the range of 20–40 μm in average. Chalcopyrite crystals were present in most of the samples in association with enargite and tennantite, forming ternary systems. Anhedral shapes were the most common ones - Fig. 3, having sizes of 20–30 μm in average. Rutile was also detected forming binary associations with quartz crystals, which identification under reflected light was possible when rutile was present. Subhedral to euhedral shapes in acicular aggregates conform the most common presentation of rutile in the samples, sized about 10–20 μm. Chalcopyrite and rutile are considered as minor minerals.

Within all the ore samples the mineralization was present either as disseminated sulphides, stockwork veins or massive with breccia and tuff textures were viewed as “principal” textures. Breccia textures result from tectonic or magmatic events, forming tectonic or hydraulic breccia. Tuff is known as generic name for extrusive pyroclastic volcanic rocks hosting the mineralization, resulting from cretaceous volcanic eruptions (Georgieva and Hikov, 2016). Stockwork texture was the predominant mineralization style identified in samples S3, S4, S5, S9 and S10. It is characterized by sulphide veins intruding the brecciated tuff matrix - Table 1.

Common mineral associations in such textures include pyrite interlocked with tennantite, enargite and chalcopyrite - Fig. 3. The veins can present widths of about 10–20 μm–1 cm thickness. The contact between veins and host rock was gradual to sharp and more than one event of intrusion could be identified in some samples. Disseminated sulphides was the predominant mineralization style in samples S2, S6, S7 and S8. It is characterized by presenting scattered sulphide crystals hosted in a tuff or brecciated tuff matrix - Table 1. Pyrite, enargite, tennantite and chalcopyrite were present in binary, ternary and more complex associations. Skeletal grains of pyrite were common in all the ore samples - Fig. 3.

2.3. Laboratory flotation

The flotation flowsheet followed at laboratory scale, resembled the one used in the plant and consisted of a bulk sulphide stage followed by copper and pyrite cleaning stages. Technological variables such as reagent dosage and conditioning time were kept constant for each test, allowing to follow samples’ chemistry and mineralogy as main variables. Before being subjected to the flotation scheme shown in Fig. 4, the sample was ground in a laboratory rod mill fitted with forged steel grinding media, targeting P80 of 90 μm which is the one maintained at the flotation plant.

The bulk sulphide flotation stage was performed inside a 4.5 L Denver cell at 25%wt. solids, whereas copper and pyrite selective stages were carried out in a 2 L cell aiming to keep pulp density constant. Bulk sulphide flotation stage was carried out at pH 8.5–9 and PAX (Potassium Amyl Xanthate) at 80 g/t was added as collector. The flotation time for the bulk stage was 13 min. Two products were obtained, a bulk sulphide concentrate and tailing - Fig. 4. All flotation tests were performed in duplicate giving a total of 20 tests for all the ten samples.

Bulk sulphide concentrate was subjected to copper selective stage at pH 12 to depress pyrite, slaked lime being used for this purpose. Formation of hydrophilic species (metal hydroxides and/or sulphoxy compounds) on pyrite surface at pH above 12 reduces its floatability (Altun et al., 2010). Copper stage was run during 11 min, where four copper concentrates were recovered at 1, 3, 6 and 11 min respectively, with two products obtained – a copper concentrate and feed for the pyrite selective stage. This latter one was realized at pH between 9 and 9.5 for 4 min. Three separate pyrite concentrates were respectively taken at 1, 2 and 4 min.

2.4. Characterization

Flotation feeds and products were assayed on-site by a laboratory managed by SGS, following methodologies described in SGS (2016) and Titley et al. (2016). The reference number of the procedure used is provided for each element mentioned like follows: Cu (ref. CON13V/AAS12B), Au (ref. FA15G/FAA25), Fe (ref. AAS40B), Ag (ref. AAS12B), As (ref. AAS40B/AAS12B) and S (ref. CSA06V). The assays were used for grade-recovery calculations. In addition, multielement 49-element assay using an ICP-MS (inductively coupled plasma mass spectrometry) was realised for the flotation feeds and tailings (ref. ICM40B).

Modal mineralogy, texture, associations, alterations and grain sizes were studied on polished blocks and grain mounts. Flotation feed samples were casted into 30 cm diameter resin mounts following an established procedure by Bouzahzah et al. (2015). The grain mounts were examined using a ZEISS Gemini Sigma 300 automated mineralogy system coupled to two Bruker xFlash 6|30 x-ray detectors and processed by ZEISS Mineralogic Mining software (Simons and Graham, 2015). The probe current was 167 μA with an acceleration voltage of 20 kV. Mineral mapping was performed in 10x10 mm sampling fields using a 3 μm step size grid at 2600× magnification. Dwell time was 0.075 s and 15,000 particles was set as measurement target, guaranteeing low statistical variance (Graham et al., 2015).

Back scattered electron (BSE) images composed by 3000 × 2000 pixels were used in post processing with the X-ray spectra as main criterion for image segmentation. Minerals were classified based on their average elemental compositions. Back-calculated elemental composition of the samples was compared to those coming from chemical assays to assess accuracy.

Table 1
Textural domains of the studied block based on observations of the samples in the current work. Alterations are described in Arizanov and Terziyski (2003), Chambefort and Moritz (2014), Georgieva and Hikov (2016) and Titley et al. (2016).

Domain	Textural characteristics	Ore Minerals	Shape	Average grain size of Cu-sulphosalts	Host rock	Alteration
Stockwork	Veinlets of 0.01–10 mm width intruding host rock in random orientations. Cu-sulphosalts interlocked with pyrite and chalcopyrite	En, Tenn, Py ± Cpy Veins also contain Qtz	Subhedral to Anhedral	1.0–6.0 mm	Breccia, Tuff	Advanced argillic with silicification/vuggy silica. Aln + Kaol + Dic are the most representative minerals
Disseminated	Scattered sulphides and Cu-sulphosalts. Cu-sulphosalts, pyrite and chalcopyrite present in binary and more complex associations	En, Tenn, Py ± Cpy	Subhedral to Anhedral	1.0–10.0 mm		

En: Enargite, Tenn: Tennantite, Py: Pyrite, Cpy: chalcopyrite, Qtz: Quartz, Kaol: Kaolinite, Dic: Dickite.

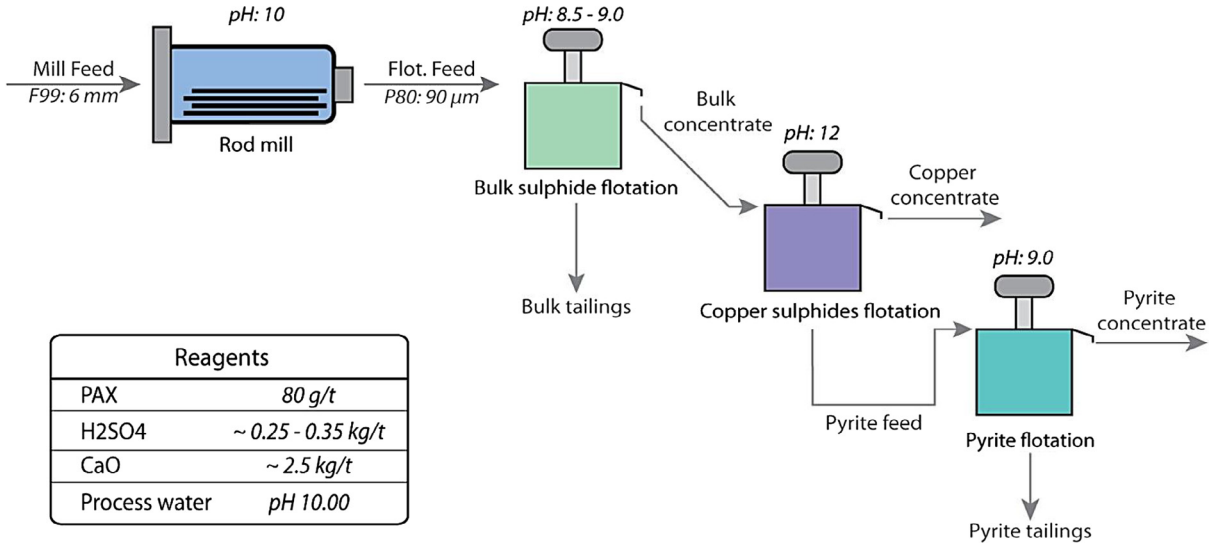

Fig. 4. Flowsheet of laboratory flotation tests.

2.5. Cu-sulphosalts recovery prediction

Principal component analysis was performed to look for relationship between mineralogical characteristics and flotation recovery for the Cu-sulphosalts. Mineral content in weight percentage as quantified by ZEISS Mineralogic in the 10 flotation feeds and flotation recovery of copper sulphosalts were used as variables. The initial variables used in the PCA are listed in Table 2. Additionally, copper deportment study was performed in order to determine which minerals and to what extent contributed to copper content of the ore.

Recovery of copper bearing minerals in each flotation product was calculated based on the grade of chalcopyrite and Cu-sulphosalts in each product relative to the respective content in the feed. Element-to-Mineral Conversion (EMC) was used to obtain the mineral composition from the chemical data. EMC is based on solving a set of linear algebraic equations represented in a matrix form where the m vector represents the weight fraction of each mineral species, C matrix represents elemental composition by mass in each mineral and a vector represents elemental composition of the sample - Eq. (2) (Lund et al., 2013; Parian et al., 2015).

$$C*m = a \tag{2}$$

As the objective is to calculate the mineralogical composition from Eq. (2), it is necessary to obtain the product of the inverse matrix C^{-1}at both sides of Eq. (2). Therefore, Eq. (3) is proposed as the solution of the system for m. Extended information about this method can be found in Whiten (2007).

$$m = C^{-1}*a \tag{3}$$

In practice, arsenic grade was used to calculate tennantite (20.37% wt. As) and enargite (19.02%wt. As) content, then the copper grade in each product was subtracted to the copper content contributed by the molecular composition of both sulphosalts (47.51%wt. Cu in tennantite and 48.41%wt. Cu in enargite). The residual copper was used to obtain the chalcopyrite (34.6%wt. Cu in molecular structure) content. Finally, pyrite content was calculated using the residual sulphur grade after subtraction of the sulphur contribution due to molecular content of sulphosalts (28.33%wt. tennantite and 32.57%wt. enargite) and chalcopyrite (34.94%wt. S).

Table 2
List of variables used for the PCA (principal component analysis).

Cu-sulphosalts (Enargite-Tennantite) (%wt.)	Recovery sulphosalts (%)
Quartz (%wt.)	Alunite (%wt.)
Pyrite (%wt.)	Rutile (%wt.)
Kaolinite/Dickite (%wt.)	Apatite (%wt.)
Chalcopyrite (%wt.)	Magnetite (%wt.)
Orthoclase (%wt.)	Gypsum (%wt.)

To find out the linear models able to predict experimental laboratory-scale flotation recovery, the samples set was subdivided into stockwork and disseminated sulphides samples. Brecciated tuff was the host texture of the ore mineralization which occurred as disseminated sulphides or stockwork veins. The general textural characteristics met in each domain are described in Table 1, commented before.

Cu-sulphosalts recovery was expressed as function of mineralogical characteristics as given by Eq. (4).

$$RS = d*X + R_0 \tag{4}$$

where

R_S: recovery of Cu-sulphosalts,
d: linear regression slope,
R_0: line intersect with ordinate axis,
X: Mineralogical variable (i.e. mineral content).

The methodology for obtaining Eq. (3) was iteratively controlled with a cross-validation step, until the model with best *RMSE* (root mean square error) and R^2 (coefficient of determination) was chosen.

3. Results and discussion

Before being subjected to a copper cleaning stage, all the samples underwent bulk sulphide flotation where have shown similar behaviour achieving a recovery above 90% at this flotation stage. Further on, an important aim was to trace the grade-recovery curves for copper at the selective (cleaning) stage. Fig. 5 summarizes the results in this direction, where each point represents a copper concentrate taken at 1, 3, 6 and 11 min. It could be noted, that copper recovery varied between 20% and 96% while grade – between 5.4% and 19%. The curve trends suggest also, that sample 1 (S1) possessed the worst performance compared to the rest of samples.

The difference in flotation performance seen in Fig. 5, could have been provoked by the mineralogical variability between the samples. Also, the pulp Eh during copper flotation can also drive such variable behavior (Greet et al., 2005; Woods, 2003). The semiconductor properties of copper bearing and copper-arsenic bearing minerals under ideal pH and Eh values determine their interaction with collectors (Lotter et al., 2016) and in such a way their flotation efficiency. The

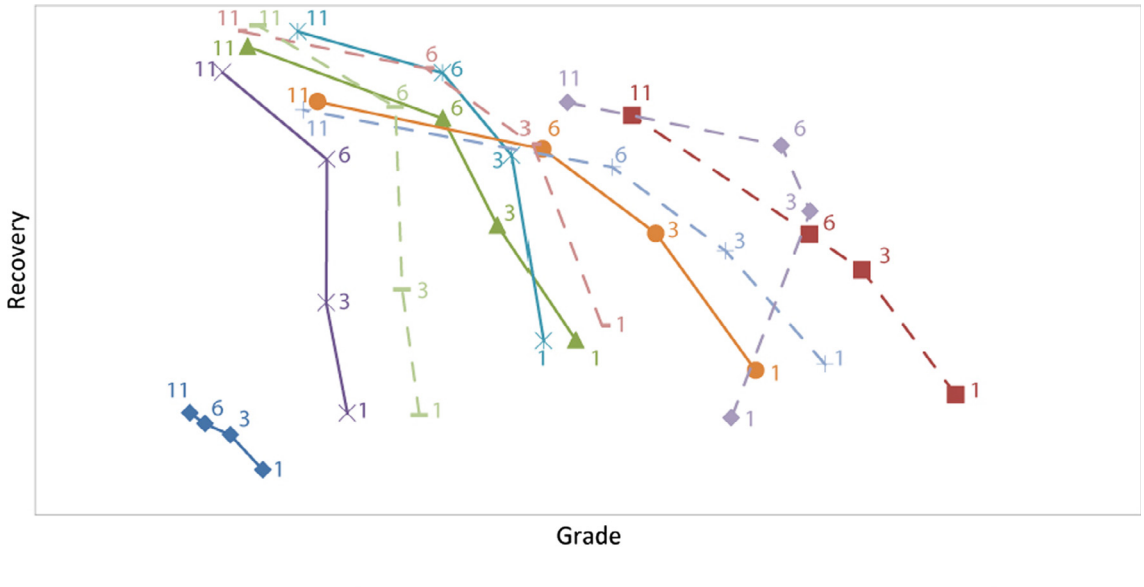

Relative Standard Deviation (RSD) of metal balance expressed in %						
ID	Cu	S	Au	Ag	As	Fe
Sample 1	2.84	5.85	0.25	8.84	5.13	7.85
Sample 2	4.48	0.06	0.64	3.75	1.29	2.59
Sample 3	2.94	9.15	0.58	3.88	6.48	7.91
Sample 4	1.24	1.31	1.73	4.76	0.77	0.99
Sample 5	4.23	1.74	2.54	15.52	1.03	7.90
Sample 6	3.24	2.75	1.74	3.51	1.85	1.61
Sample 7	0.95	4.50	1.59	24.13	7.03	0.78
Sample 8	5.76	0.85	0.68	10.05	8.48	4.14
Sample 9	3.43	2.28	7.08	7.15	2.84	3.63
Sample 10	1.63	3.65	0.49	9.69	8.53	1.96

Fig. 5. Cu grade vs. recovery in the copper cleaner under optimized flotation conditions for all samples*. Numbers express the flotation time (min) for the collected concentrate. Dashed and continuous lines represent samples with disseminated sulphides and stockwork mineralization respectively. Relative standard deviation (RSD) values of the metal balance for the flotation tests are presented (*Precise values are not communicated due to confidentiality).

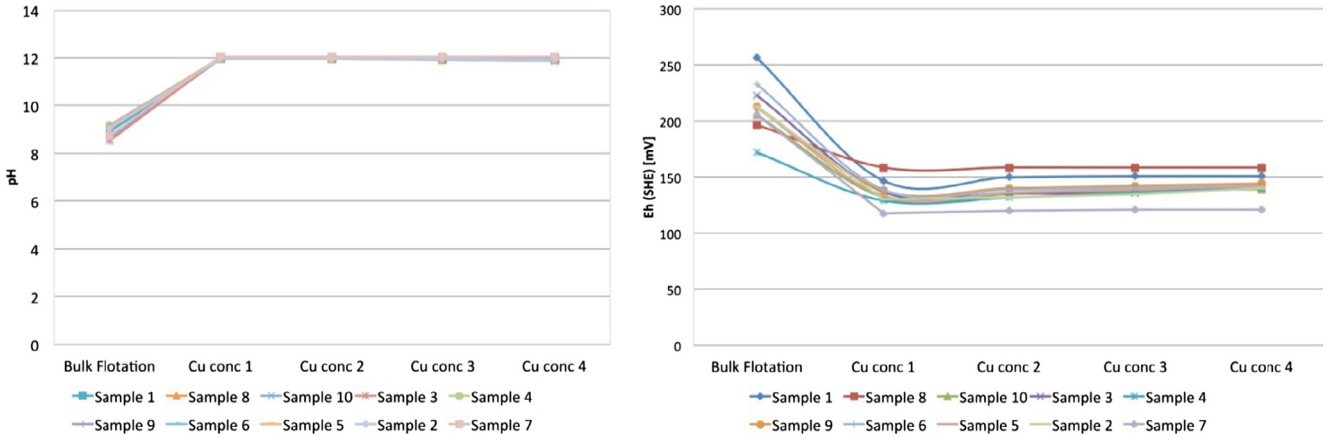

Fig. 6. Pulp pH (left) and Eh (right) for the 10 samples during bulk sulphide flotation under optimized conditions.

ideal Eh and pH ranges for enargite flotation are respectively: −150 < Eh < 516 mV SHE (Standard Hydrogen Electrode) and 8 < pH < 11 (Plackowski et al., 2014; Senior et al., 2006). For tennantite these are respectively, 150 < Eh < 250 mV SHE and 8 < pH < 12 (Smith et al., 2012). For chalcopyrite these are, 0 < Eh < 200 and 6 < pH < 10 (Fuerstenau et al., 2007; Heyes and Trahar, 1979). Flotation at "non-ideal" Eh windows and pH values tends to deteriorate the grade-recovery signature. Fig. 6 illustrates the pH and Eh values recorded during bulk and copper selective stages. The immediate impression is that pH was maintained stable throughout all the tests. Eh however show some variations during copper cleaner stage, ranging between 120 mV (Sample 7) and 158 mV (S8). The

Table 3
Modal mineralogy of the 10 samples used as flotation feed.

Mineralization type	Stockwork					Disseminated sulphides				
Minerals (%wt.)	Sample 1	Sample 3	Sample 4	Sample 9	Sample 10	Sample 2	Sample 5	Sample 6	Sample 7	Sample 8
Quartz	57.2	54.4	63.8	42.7	49.6	60.9	57.3	38.3	61.3	53.6
Pyrite	22.9	31	20.5	28.7	25.3	26.6	15.1	34.7	23.7	20
Kaolinite	18.5	11.1	11	25.3	20.8	6.1	24.3	23	11.2	23.8
Cu-sulphosalts	0.2	1.9	3	1.7	2.3	3.4	1.7	1.8	2.1	0.8
Famatinite	0.03	0	0	0	0	0	0	0	0	0
Chalcopyrite	0.2	0.9	0.5	0.9	0.8	2.1	0.3	0.9	0.5	0.4
Alunite	0.6	0	0.4	0.2	0.5	0.2	0.5	0.6	0.3	0.7
Rutile	0.2	0.3	0.3	0.2	0.2	0.3	0.3	0.3	0.3	0.2
Apatite	0	0.2	0.3	0.2	0.3	0.3	0.4	0.2	0.5	0.4
Magnetite	0.1	0.1	0	0.1	0.2	0.1	0.1	0.1	0	0.1
Barite	0	0	0	0	0	0	0	0	0	0
Gypsum	0	0	0	0	0	0	0	0	0	0
Orthoclase	0	0.1	0.1	0	0	0	0	0	0	0.1
Total	100	100	100	100	100	100	100	100	100	100

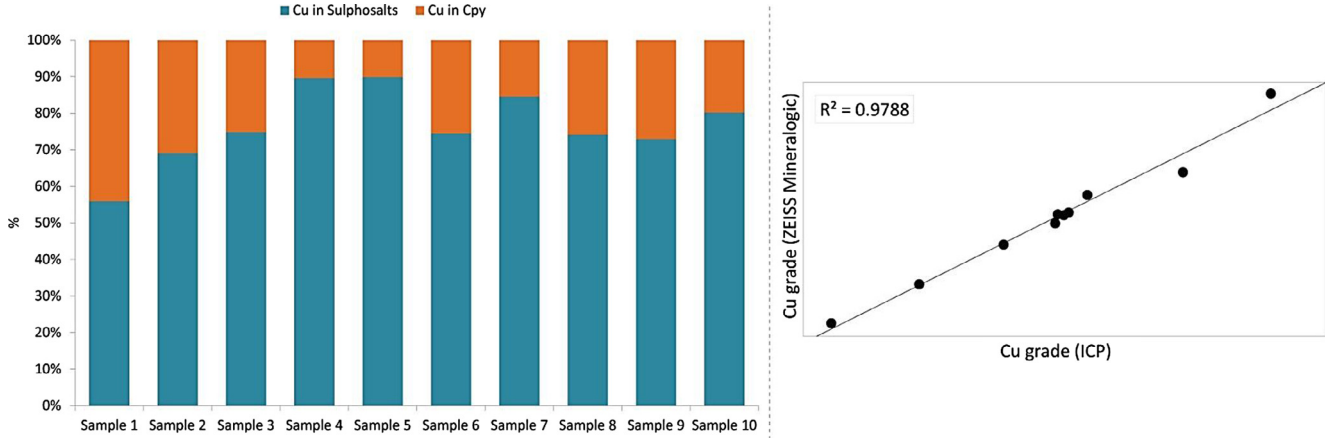

Fig. 7. Left: Relative copper distribution in sulphosalts and chalcopyrite for the flotation feed samples. Right: cross-validation between copper from ICP assays and back-calculated from ZEISS Mineralogic results.

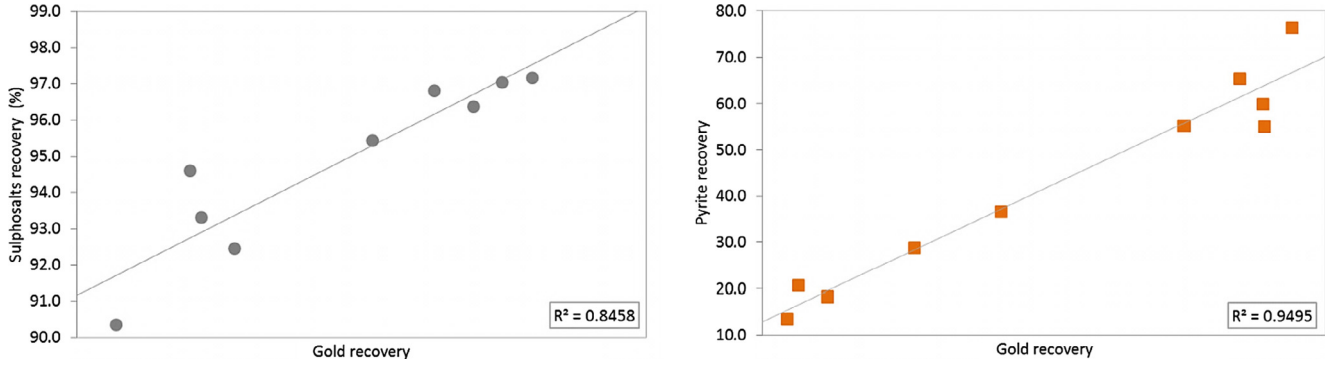

Fig. 8. Correlation between recovery of Cu-sulphosalts' and gold in the copper cleaning stage (left), and gold and pyrite recovery in the pyrite cleaning stage (right).

observed Eh values in the copper cleaner, match well with the recommended intervals for chalcopyrite and enargite, but only two tests matched the one for tennantite (S1 and S8), with the lowest being 120 mV corresponding to S7. However, this slight shift did not influence the overall recovery-grade performances for copper (Fig. 5), as S1 presented the worst performance compared to S7 and S8. Tennantite flotation was likely possible outside the Eh window as suggested by Smith et al. (2012). It should be noted that literature related to tennantite flotation is rather sparse.

Released iron ions in solution resulting from the forged steel rods, could have also influenced the depression of copper sulphides and acidity, as Fe^{3+} ions consume available oxygen to form OH compounds that precipitate on the minerals surface, decreasing the pH (Chen et al., 2013; Gonçalves et al., 2003; Jacques et al., 2016; Peng et al., 2012). Some authors (Gonçalves et al., 2003; Peng and Grano, 2010; Yelloji Rao and Natarajan, 1988) have suggested that grinding media that favors reducing environments is detrimental for copper sulphide flotation. Lime addition during grinding stage was crucial in view limiting the influence of such phenomenon. In this context, the use of an inert grinding media (e.g. Cr-dotted steel rods) would have helped to eliminate these effects, but such media was unavailable during the experimental program.

The modal mineralogy for the ten flotation feeds is presented in Table 3. Quartz, pyrite and kaolinite represented more than 95%wt. of

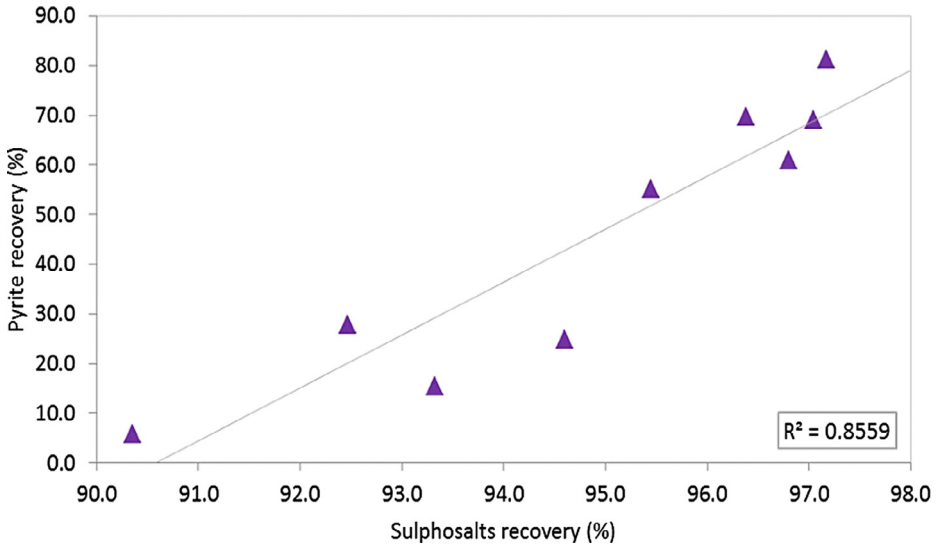

Fig. 9. Relationship between recovery of Cu-sulphosalts and pyrite at the copper cleaning stage.

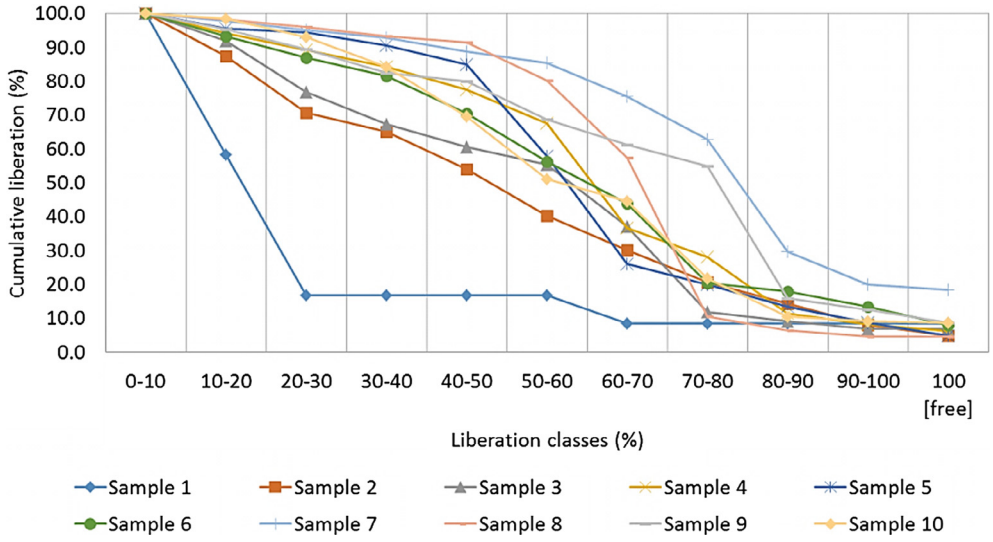

Fig. 10. Cumulative liberation curves for the Cu-sulphosalts in the 10 flotation feeds.

the minerals being present. The Cu-sulphosalts, composed of luzonite, enargite and tennantite are the most abundant copper mineral group, followed by chalcopyrite. Cu-sulphosalts varied from 0.01%wt. (Sample 1) to 3.4%wt. (Sample 2). The figures for chalcopyrite were as high as 0.9 %wt. (samples 3, 6 and 9). On average, quartz was present in 53.9% wt., pyrite in 24.9%wt., kaolinite in 17.5%wt., and Cu-sulphosalts in 1.9%wt.

Fig. 7 illustrates the copper deportment results. In general, Cu-sulphosalts accounted for more than half of the copper available in the samples. Copper due to chalcopyrite was the highest in Sample 1 and less than 40% in the remaining nine samples (Fig. 7 - left). Cross – validation between copper measured by ICP and back-calculated from ZEISS Mineralogic presented a R^2 value of 0.98 and a RMSE of 0.1% (Fig. 7 - right).

Although gold was identified in the flotation feeds by fire assay, it was not possible to be detected neither by optical inspection nor by automated mineralogy. This suggests that, more likely, it is present as inclusions in pyrite' crystalline structure and not as interlocked with enargite, tennantite or pyrite as usually occurs in other blocks of the Chelopech deposit (Bonev et al., 2002). To assess this hypothesis, graphs of mineral recovery vs. gold recovery were plotted - Fig. 8. It was found out, that gold recovery (data not reported due to nature of project) correlated well with both Cu-sulphosalts and pyrite recovery, giving a R^2 of 0.85 and 0.95 respectively. Although the R^2 coefficient was higher for the pyrite recovery, no clear association of gold solely to the former or to the latter could be inferred. In addition, it is known that the arsenic content in copper sulphosalts and pyrite strongly favours gold content in their crystalline structures (Dunne et al., 2009; John et al., 2013). Past studies on gold deportment in the Chelopech mine have shown that pyrite can carry inside its crystalline structure up to 1% arsenic (Arizanov and Terziyski, 2003; Chambefort and Moritz, 2014) and up to 45% of the gold present in the Chelopech deposit is refractory (Bonev et al., 2002). This clearly supports the statement that gold floats together with pyrite and copper sulphosalts as refractory gold.

Fig. 9 illustrates the literally linear correlation between the Cu-sulphosalts and pyrite recoveries at the copper cleaning stage. The fact that pyrite floated in the copper cleaning stage can be due to its non-satisfactory depression or to mineralogical associations such as pyrite locked with Cu-sulphosalts.

Cumulative liberation curves for Cu-sulphosalts were constructed from the automated mineralogy results and are shown in Fig. 10. Samples S7 and S9 were the ones showing the best liberation degree, with nearly 60–70% of the Cu-sulphosalt grains achieving at least

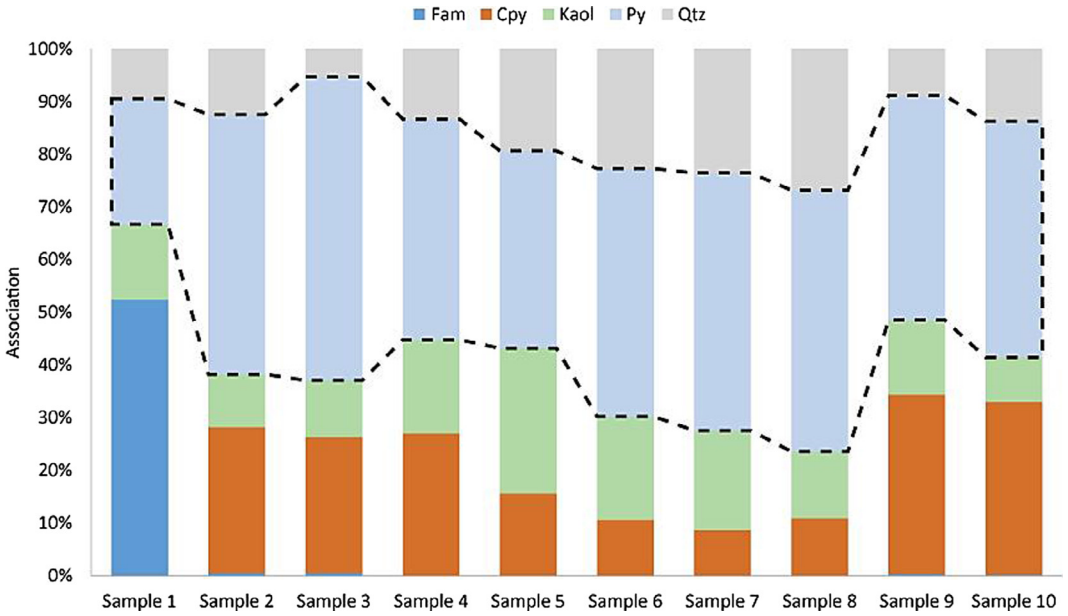

Fig. 11. Relative association of the minerals to Cu-sulphosalts. Pyrite was the main phase associated with enargite and tennantite (dashed line). Fam: famantinite, Cpy: Chalcopyrite, Kaol: Kaolinite + dickite, Py: Pyrite, Qtz: Quartz.

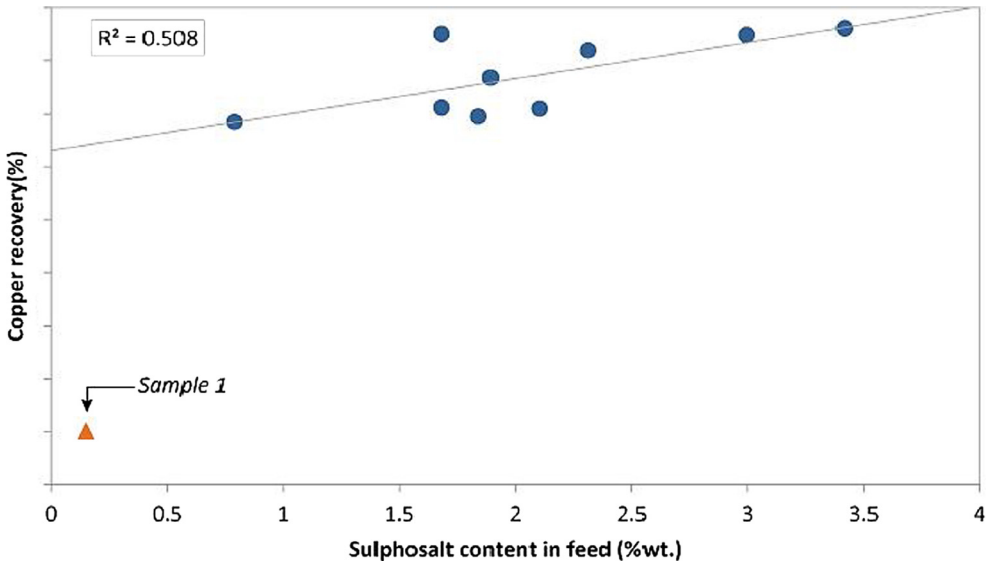

Fig. 12. Copper recovery as a function of Cu-sulphosalts content in the feed. The sample 1 presented the lowest recovery values due to low enargite and tennantite content.

70–80% liberated surface. Otherwise, the rest of the samples presented less than 30% liberation degree for the same class. When analysing the shape of the curve for sample 1 (S1), one could notice that it differs to the curves of the rest ones. This can be explained by the lesser amount of identified Cu-sulphosalts' grains in S1 being lower than 100 and giving lower statistical representativeness and hence inaccurate liberation results.

In addition to the liberation data, the relative association of the main mineral phases with the Cu-sulphosalts, as pictured in Fig. 11, allowed to identify pyrite as the most associated to the Cu-sulphosalts phase, with up to 50% of associated grains (S3). Chalcopyrite was the second most associated phase, with proportions ranging from 30% (S9) to 8% (S7). The gangue minerals associated with Cu-sulphosalts were mainly quartz and kaolinite (Fig. 11). These results confirm that pyrite recovery in the copper cleaning stage was facilitated by interlocking due to the low liberation degree of the both minerals in the feed.

Copper recovery was plotted against the Cu-sulphosalts content (in %wt.) and results displayed in Fig. 12. Out of 10 samples, 9 followed a linear trend with coefficient of determination R^2 of 0.508. On the other hand, S1 came out a bit displaced from the main stream, showing both low copper recovery and Cu-sulphosalts content. The correlation seen in Fig. 12 suggests that the content of Cu-sulphosalts do control the copper recovery in the copper cleaning circuit, with S1 having the worst performance due to its low grade in Cu-bearing minerals. However, due to the use of PAX as collector and the clear pyrite-enargite-tennantite association, one could not neglect the possibility that the sulphosalts might be recovered thanks to their interlockings with the hydrophobic pyrite.

The PCA results confirmed the findings suggested by the results shown in Fig. 12. The loading plot of principal components 1 and 2 (PC1, PC2) having more than 50% variance contribution - Fig. 13, shows that the recovery of Cu-sulphosalts together with Cu-sulphosalts

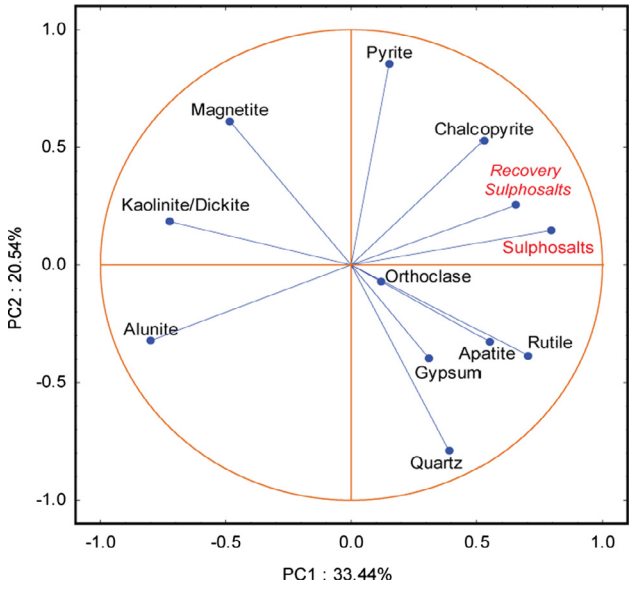

Fig. 13. Loading plot of mineral content with Cu-sulphosalts recovery in the principal component 1 (PC1) vs. PC2 vector plane.

Table 4
Samples grouped as belonging to the two textural domains.

Sample ID	Type of material	Lithology	Mineralization style
Sample 1	Chip – Sample	Brecciated tuff	Stockwork
Sample 2	Drill core	Brecciated tuff	Disseminated sulphides
Sample 3	Drill core	Brecciated tuff	Stockwork
Sample 4	Drill core	Brecciated tuff	Stockwork
Sample 5	Drill core	Brecciated tuff	Disseminated sulphides
Sample 6	Drill core	Brecciated tuff	Disseminated sulphides
Sample 7	Chip – sample	Brecciated tuff	Disseminated sulphides
Sample 8	Chip – sample	Brecciated tuff	Disseminated sulphides
Sample 9	Drill core	Brecciated tuff	Stockwork
Sample 10	Chip – sample	Brecciated tuff	Stockwork

content presented the largest contribution in the PC1, with eigenvectors of 0.65 and 0.80 respectively. In such a way, the correlation between the Cu-sulphosalts content (in %wt.) and the Cu-sulphosalts recovery could be outlined. Variance contribution from additional mineralogical characteristics (e.g. grain size) to sulphosalts recovery was not observed in any other principal component.

In line with the methodology being followed, the above-mentioned results were further processed to create models aiming to predict Cu-sulphosalts recovery. To fulfil this task, Table 4 was created where stockwork mineralization being conferred to samples S1, S3, S4, S9 and S10 and disseminated sulphides mineralization - to S2, S5, S6, S7 and S8. As a consequence, two equations (one per mineralization domain) were proposed for the studied block. They are presented in Fig. 14, together with the cross–validation results for the experimental and predicted recoveries, found as RMSE 1.32% and R^2 0.6508 respectively.

4. Conclusions

The results reaffirm the practicability of using a simple geometallurgical testing procedure in studying the flotation behaviour of Cu-bearing minerals. In our case, the classification of a mining block into geometallurgical domains and their characterization allow to better understand the flotation behaviour of the Cu-sulphosalts present in the studied block. While the study has been focused on the Chelopech deposit, the methodology could be used as convenient and efficient tool in other mining projects dealing with similar mineralisation.

The following major conclusions could be derived from the presented results:

Based on the textural characteristics of the samples, two geological domains could be proposed in the studied block: one with sulphides precipitating in veinlet forms (stockwork) and the other - in disseminated grains. PCA and flotation results suggested similar Cu-sulphosalts recovery for these domains. However, modelling of Cu-sulphosalts recovery based on Cu-sulphosalts content has to be done separately by grouping the samples according to domain belonging. Cu-sulphosalts accounted for nearly 77% of the copper available in the tested samples with their content being directly correlated to copper recovery. Mean square errors were found rather high, but are expected to improve with more samples being gathered and tested.

Since SEM–based automated mineralogy equipment is not available

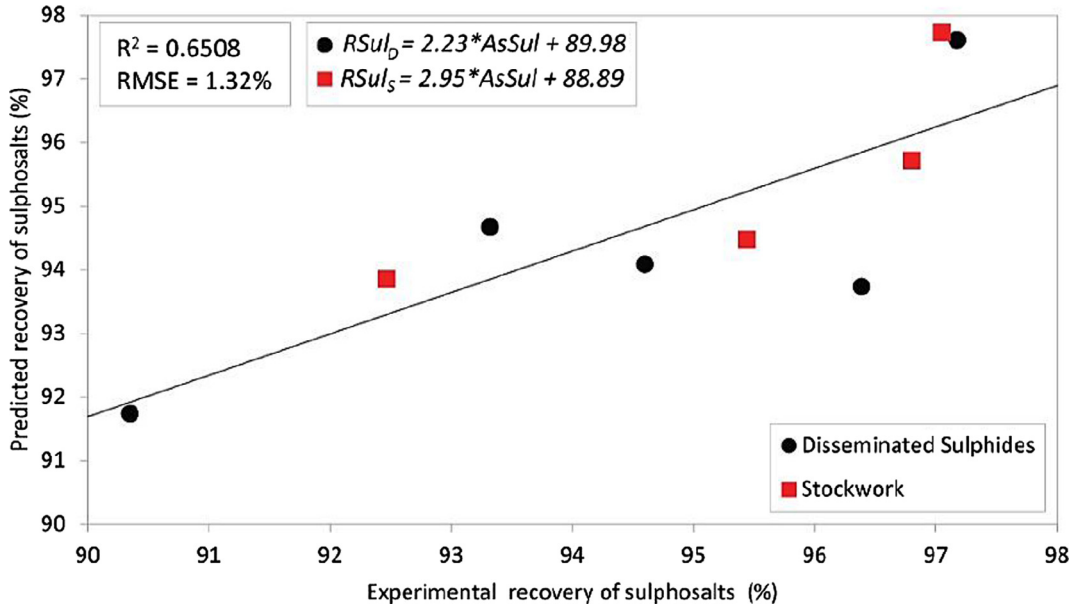

Fig. 14. Comparison between experimental and predicted values for Cu-sulphosalts recovery (RSul) in the copper cleaning stage. AsSul: %wt. of enargite and tennantite in the feed, c, b: constants, S: Stockwork, D: Disseminated sulphides.

at mill site, the weight percentage of Cu-sulphosalts obtained using element to mineral conversion could be used as rapid means enabling mineral quantification.

Gold is believed to be found as inclusions below 1 µm, possibly present as solid solution inside the pyrite crystal structure. Gold recovery in the copper cleaning stage is assumed to has been largely influenced by interlocking and associations between pyrite and Cu-sulphosalts.

Acknowledgements

The authors would like to thank Dr Hassan Bouzahzah for the automated mineralogy and DPM-Chelopech for the permission to use project results and deliver an article. Thanks should go also to the anonymous reviewers whose suggestions improved the quality of the present research publication.

References

Altun, N., Güler, T., Akdemir, Ü., 2010. Pyrite flotation: a review. In: Proceedings of the XIIth International Mineral Processing Conference, Cappadochia-Nevşehir, Turkey, pp. 295–303.

Arizanov, A., Terziyski, S., 2003. The Chelopech Cu-Au deposit. In: Bogdanov, K., Strashimirov, S. (Eds.), Cretaceous Porphyry-Epithermal Systems of the Srednogorie Zone. Society of Economic Geologists, Bulgaria, pp. 79–89.

Bonev, I.K., Kerestedjian, Æ.T., Atanassova, R., Andrew, Æ.C.J., 2002. Morphogenesis and composition of native gold in the Chelopech volcanic-hosted Au – Cu epithermal deposit, Srednogorie zone, Bulgaria. Miner. Depos. 614–629. https://doi.org/10.1007/s00126-002-0273-8.

Bouzahzah, H., Benzaazoua, M., Mermillod-Blondin, R., Pirard, E., 2015. A novel procedure for polished section preparation for automated mineralogy avoiding internal particle settlement. 12th International Congress for Applied Mineralogy (ICAM), 10–12 August 2015, Istanbul, Turkey.

Chambefort, I., Moritz, R., 2014. Subaqueous environment and volcanic evolution of the Late Cretaceous Chelopech Au – Cu epithermal deposit, Bulgaria. J. Volcanol. Geotherm. Res. 289, 1–13. https://doi.org/10.1016/j.jvolgeores.2014.10.013.

Chen, X., Peng, Y., Bradshaw, D., 2013. Effect of regrinding conditions on pyrite fl otation in the presence of copper ions. Int. J. Miner. Process. 125, 129–136. https://doi.org/10.1016/j.minpro.2013.08.007.

Dundee Precious Metals Inc., 2017. Dundee Precious Metals Announces Second Quarter 2017 Production Results [WWW Document]. Press Release. < http://www.dundeeprecious.com/English/Corporate-News/press-release-details/2017/Dundee-Precious-Metals-Announces-Second-Quarter-2017-Production-Results/default.aspx > (accessed 2.16.17).

Dunne, R., Levier, M., Acar, S., Kappes, R., 2009. Keynote Address: Newmont's contribution to gold technology. In: World Gold Conference 2009. The Southern African Institute of Mining and Metallurgy, Johannesburg, pp. 221–230.

Dzvinamurungu, T., Viljoen, K.S., Knoper, M.W., Mulaba-bafubiandi, A., 2013. Geometallurgical characterisation of Merensky Reef and UG2 at the Marikana Mine, Bushveld Complex, South Africa. Miner. Eng. 52, 74–81. https://doi.org/10.1016/j.mineng.2013.04.010.

Farrokhpay, S., Fornasiero, D., 2017. Flotation of coarse composite particles: effect of mineral liberation and phase distribution. Adv. Powder Technol. 28, 1849–1854. https://doi.org/10.1016/j.apt.2017.03.012.

Fuerstenau, M.C., Yoon, R.-H., Jameson, G.J., 2007. Froth Flotation: A Century of Innovation. Society for Mining, Metallurgy, and Exploration – SME.

Georgieva, S., Hikov, A., 2016. Geochemistry of hydrothermally altered rocks from the Chelopech high sulphidation Cu-Au deposit, Bulgaria. Доклади на Българската академия на науките 69, 10.

Georgieva, S., Velinova, N., 2014. Florencite - (ce , la , nd) and crandallite from the advanced argillic alteration in the chelopech high-sulphidation epithermal cu-au deposit, Bulgaria. Comptes rendus l'Academie Bulg. des Sci. 67, 1669–1678.

Georgieva, S., Velinova, N., Petrunov, R., Chambefort, I., 2002. Aluminium phosphate-sulphate minerals in the Chelopech Cu-Au deposit: Spatial development, chemistry and genetic significance. Geochem. Miner. Petrol. 39, 39–51.

Gonçalves, K.L., Andrade, V.L.L., Peres, A.E.C., 2003. The effect of grinding conditions on the flotation of a sulphide copper ore. Miner. Eng. 16, 1213–1216. https://doi.org/10.1016/j.mineng.2003.05.006.

Graham, S., Brough, C., Cropp, A., 2015. An Introduction to ZEISS Mineralogic Mining and the correlation of light microscopy with automated mineralogy: a case study using BMS and PGM analysis of samples from a PGE- bearing chromitite prospect.

Greet, C.J., Kinal, J., Steinier, P., 2005. Grinding media – its effect on pulp chemistry and flotation behaviour. In: Proceedings Centenary of Flotation, Brisbane, pp. 967–972.

Gy, P.M., 1995. Introduction to the theory of sampling I. Heterogeneity of a population of uncorrelated units. TrAC Trends Anal. Chem. 14, 67–76. https://doi.org/10.1016/0165-9936(95)91474-7.

Gy, P.M., 1976. The sampling of particulate materials — a general theory. Int. J. Miner. Process. 3, 289–312. https://doi.org/10.1016/0301-7516(76)90020-X.

Heyes, G.W., Trahar, W.J., 1979. Oxidation-reduction effects in the flotation of chalcocite and cuprite. Int. J. Miner. Process. 6, 229–252. https://doi.org/10.1016/0301-7516(79)90039-5.

Jacques, S., Greet, C.J., Bastin, D., 2016. Oxidative weathering of a copper sulphide ore and its influence on pulp chemistry and flotation. Miner. Eng. 99, 52–59. https://doi.org/10.1016/j.mineng.2016.09.023.

John, J., Johnson, N.W., Stewart, K., Turner, D., Bradshaw, D., 2013. A review of pre-treatment methods to separate the different types of pyrites in gold processing. In: Proceedings World Gold 2013. The Australasian Institute of Mining and Metallurgy, Melbourne, pp. 347–356.

Keeney, L., Walters, S., 2009. Development of Geometallurgical Comminution Mapping and Modelling. In: 41st Annu. Meet. Can. Miner. Process. January 20, Ottawa, Ontario, Canada, pp. 19.

Keeney, L.M., 2010. The development of a novel method for integrating geometallurgical mapping and orebody modelling. Univ. Queensl. 309, pages.

Lishchuk, V., 2016. Geometallurgical Programs – Critical Evaluation of Applied Methods and Techniques. Dep. Civil, Environ. Nat. Resour. Eng. Luleå Univ. Technol. (126 pages).

Lopera Montoya, P.A., 2014. Geometallurgical Mapping and Mine Modelling – Comminution Studies: La Colosa Case Study. AMIRA P843A. Univ., Tasmania (88 pages).

Lotter, N.O., 2011. Modern process mineralogy: an integrated multi-disciplined approach to flowsheeting. Miner. Eng. 24, 1229–1237. https://doi.org/10.1016/j.mineng.2011.03.004.

Lotter, N.O., Bradshaw, D.J., Barnes, A.R., 2016. Classification of the Major Copper Sulphides into semiconductor types, and associated flotation characteristics. Miner. Eng. 96–97, 177–184. https://doi.org/10.1016/j.mineng.2016.05.016.

Lotter, N.O., Bradshaw, D.J., Becker, M., Parolis, L.A.S., Kormos, L.J., 2008. A discussion of the occurrence and undesirable flotation behaviour of orthopyroxene and talc in the processing of mafic deposits. Miner. Eng. 21, 905–912. https://doi.org/10.1016/j.mineng.2008.02.023.

Lotter, N.O., Kormos, L.J., Oliveira, J., Fragomeni, D., Whiteman, E., 2011. Modern process mineralogy: two case studies. Miner. Eng. 24, 638–650. https://doi.org/10.1016/j.mineng.2011.02.017.

Lund, C., Lamberg, P., Lindberg, T., 2013. Practical way to quantify minerals from chemical assays at Malmberget iron ore operations – an important tool for the geometallurgical program. Miner. Eng. 49, 7–16. https://doi.org/10.1016/j.mineng.2013.04.005.

McKay, N.A., Wilson, S.W., Lacouture, B., 2007. Ore characterisation of the aqqaluk deposit at red dog. In: Canadian Mineral Processors 39th, Ottawa, Canada, pp. 55–74.

Mena, C., 2015. Kinetic and Process Mineralogical Studies Upon the Bulk Sulphide Flotation Circuit at Dundee Precious Metals – Chelopech Concentrator in Bulgaria. Univ. Liège (102 pages).

Moëlo, Y., Makovicky, E., Mozgova, N.N., Jambor, J.L., Cook, N., Pring, A., Paar, W., Nickel, E.H., Graeser, S., Karup-Møller, S., Balic-Žunic, T., Mumme, W.G., Vurro, F., Topa, D., 2008. Sulfosalt systematics: a review. Report of the sulfosalt sub-committee of the IMA Commission on Ore Mineralogy. Eur. J. Miner. 20, 7–62. https://doi.org/10.1127/0935-1221/2008/0020-1778.

Moritz, R., Chambefort, I., Georgieva, S., Jacquat, S., Petrunov, R., 2005. 3–2: The Chelopech high-sulphidation epithermal Cu–Au deposit. Ore Geol. Rev. 27, 130–131. https://doi.org/10.1016/j.oregeorev.2005.07.021.

Naumov, D., 2016. Possibilities for Increased Recovery of Copper and Precious Metals Bearing Minerals at the Bulk and Copper Selective Flotation Stages at Chelopech Concentrator, Bulgaria. Univ. Liège (146 pages).

Ntlhabane, S., Becker, M., Charikinya, E., Voigt, M., Schouwstra, R., Bradshaw, D., 2018. Towards the development of an integrated modelling framework underpinned by mineralogy. Miner. Eng. 116, 123–131. https://doi.org/10.1016/j.mineng.2017.09.013.

Parian, M., Lamberg, P., Möckel, R., Rosenkranz, J., 2015. Analysis of mineral grades for geometallurgy: combined element-to-mineral conversion and quantitative X-ray diffraction. Miner. Eng. 82, 25–35. https://doi.org/10.1016/j.mineng.2015.04.023.

Peng, Y., Grano, S., 2010. Effect of grinding media on the activation of pyrite flotation. Miner. Eng. 23, 600–605. https://doi.org/10.1016/j.mineng.2010.02.003.

Peng, Y., Wang, B., Gerson, A., 2012. The effect of electrochemical potential on the activation of pyrite by copper and lead ions during grinding. Int. J. Miner. Process. 102–103, 141–149. https://doi.org/10.1016/j.minpro.2011.11.010.

Plackowski, C., Bruckard, W.J., Nguyen, A.V., 2014. Surface characterisation, collector adsorption and flotation response of enargite in a redox potential controlled environment. Miner. Eng. 65, 61–73. https://doi.org/10.1016/j.mineng.2014.05.013.

Senior, G.D., Guy, P.J., Bruckard, W.J., 2006. The selective flotation of enargite from other copper minerals — a single mineral study in relation to beneficiation of the Tampakan deposit in the Philippines. Int. J. Miner. Process. 81, 15–26. https://doi.org/10.1016/j.minpro.2006.06.001.

SGS, 2016. SGS Analytical Services Guide.

Simons, B., Graham, S., 2015. ZEISS Mineralogic Mining: Iron Oxide Analysis by Automated Mineralogy.

Smith, A.J.B., Viljoen, K.S., Schouwstra, R., Roberts, J., Schalkwyk, C., Gutzmer, J., 2013. Geological variations in the Merensky Reef at Bafokeng Rasimone Platinum Mine and its influence on flotation performance. Miner. Eng. 52, 155–168. https://doi.org/10.1016/j.mineng.2013.05.015.

Smith, L.K., Davey, K.J., Bruckard, W.J., 2012. The use of pulp potential control to separate copper and arsenic – an overview based on selected case studies. In: Proceedings XXVI International Mineral Processing Congress – IMPC, New Delhi, pp. 5057–5067.

Stoykov, S., Peytcheva, I., Von Quadt, A., Moritz, R., Frank, M., Fontignie, D., 2004. Timing and magma evolution of the Chelopech volcanic complex (Bulgaria). Schweizerische Mineral. und Petrogr. Mitteilungen 101–117.

Suazo, C.J., Kracht, W., Alruiz, O.M., 2010. Geometallurgical modelling of the Collahuasi

flotation circuit. Miner. Eng. 23, 137–142. https://doi.org/10.1016/j.mineng.2009.11.005.
Titley, M., Meik, S., Overall, R., White, G., Kuzmanova, P., 2016. Dundee Precious Metals Inc. - NI 43–101 Technical Report Mineral Reserve Update – Chelopech Project. Chelopech, Bulgaria.
Tungpalan, K., Manlapig, E., Andrusiewicz, M., Keeney, L., Wightman, E., 2015a. An integrated approach of predicting metallurgical performance relating to variability in deposit characteristics. Miner. Eng. 71, 49–54. https://doi.org/10.1016/j.mineng.2014.10.004.
Tungpalan, K., Wightman, E., Manlapig, E., 2015b. Relating mineralogical and textural characteristics to flotation behaviour. Miner. Eng. 82, 136–140. https://doi.org/10.1016/j.mineng.2015.02.005.
Wang, W., Fornasiero, D., 2010. Flotation of composite synthetic particles. In: XXV International Mineral Processing Congress 2010, IMPC 2010, Brisbane, QLD, pp. 2503–2511.
Whiteman, E., Lotter, N.O., Amos, S.R., 2016. Process mineralogy as a predictive tool for flowsheet design to advancethe Kamoa project. Miner. Eng. 96–97, 185–193. https://doi.org/10.1016/j.mineng.2016.05.004.
Whiten, B., 2007. Calculation of mineral composition from chemical assays. Miner. Process. Extr. Metall. Rev. 29, 83–97. https://doi.org/10.1080/08827500701257860.
Woods, R., 2003. Electrochemical potential controlling flotation. Int. J. Miner. Process. 72, 151–162. https://doi.org/10.1016/S0301-7516(03)00095-4.
Yelloji Rao, M.K., Natarajan, K.A., 1988. Electrochemical aspects of grinding media-mineral interaction on sulphide flotation. Bull. Mater. Sci 10, 411–422.
Zhang, J., Subasinghe, N., 2016. Development of a flotation model incorporating liberation characteristics. Miner. Eng. 98, 1–8. https://doi.org/10.1016/j.mineng.2016.05.021.